



Disruption of the nucleoporin gene *NUP133* results in clustering of nuclear pore complexes

LUCY F. PEMBERTON, MICHAEL P. ROUT, AND GÜNTER BLOBEL

Laboratory of Cell Biology, Howard Hughes Medical Institute, The Rockefeller University, New York, NY 10021

Contributed by Günter Blobel, October 3, 1994

ABSTRACT We have characterized a protein with an estimated molecular mass of 130 kDa that is contained in a highly enriched yeast nuclear pore complex (NPC) fraction. Partial amino acid sequence from this protein has led us to a previously identified open reading frame on chromosome XI of *Saccharomyces cerevisiae* encoding a protein of 133 kDa. Due to its coenrichment with NPCs during cell fractionation and the phenotype observed in the disrupted strain, we propose to term the gene encoding this protein *NUP133*. Cells carrying a disrupted copy of *NUP133* were temperature sensitive for growth. In addition, abnormal clustering of NPCs was observed. This phenotype is similar to that previously observed in the disruption of another nucleoporin gene, *NUP145*. We speculate that the gene product of *NUP133*, Nup133p, may functionally overlap with the *NUP145* gene product, Nup145p, and that these proteins may be involved in maintaining the position of the NPC within the nuclear envelope.

Nuclear pore complexes (NPCs) are large, proteinaceous structures in the eukaryotic nuclear envelope through which occurs the active transport of macromolecules between the nucleus and the cytoplasm (reviewed in refs. 1–3). Individual polypeptide components of the NPC, referred to as nucleoporins, have been identified in both vertebrates and the yeast *Saccharomyces* (1). Several of the nucleoporins so far identified have fallen into distinct subsets on the basis of repeated amino acid motifs. The relevance of these repeated motifs to function is not yet understood. Although some sequence similarities between the vertebrate and yeast NPC proteins exist, functional homologs have yet to be identified (1).

Highly enriched NPC fractions have been prepared from yeast (4). These procedures indicate that the yeast NPC may comprise as many as 80 different polypeptides. To date, the genes of only eight nucleoporins have been identified in yeast. These nucleoporins can be divided into three distinct families: those containing XFXFG amino acid repeats (5–7), those with multiple repeats of the tetrapeptide GLFG (8–11), and those lacking any repetitive motifs (12). In addition, a protein of the pore membrane domain, Pom152p, has been shown to be a component of the highly enriched NPC fraction (13). Some of the nucleoporins are not essential for viability, indicating some redundancy within the NPC (1). Interesting abnormalities in the nuclear envelope structure have been observed with disruptions of two nucleoporin genes (10, 14).

The isolation and characterization of a gene for another nucleoporin is described here. Biochemical analysis demonstrates that this protein cofractionates with other components of the NPC. Disruption of the gene for this protein leads to striking clustering of NPCs in the nuclear envelope.

The publication costs of this article were defrayed in part by page charge payment. This article must therefore be hereby marked "advertisement" in accordance with 18 U.S.C. §1734 solely to indicate this fact.

MATERIALS AND METHODS

Fractionation of Yeast Nuclear Proteins. Proteins from a preparation of highly enriched yeast NPCs (10 mg of total protein) were fractionated by ion-exchange chromatography, reverse-phase HPLC, and SDS/PAGE as described (4). Fractions containing a 130-kDa doublet were electrophoretically transferred to polyvinylidene difluoride membrane (PVDF) and visualized with 0.1% amido black in 10% (vol/vol) acetic acid. Both bands of the 130-kDa doublet were excised together and cleaved with endoproteases. N-terminal sequence analysis was performed on several internal peptides (15, 16).

Peptide Antiserum Production. A 15-amino acid peptide corresponding to amino acids 1121–1135 (ETLNSDNLSEIKLHS) was synthesized, coupled to keyhole limpet hemocyanin, and used to immunize rabbits (Genosys, The Woodlands, TX). Rabbit serum was affinity purified by using immunizing peptide coupled to Affi-Gel-15 (Bio-Rad) according to the manufacturer's instructions.

Western Blot Analysis. Proteins were separated by SDS/PAGE and transferred to nitrocellulose. Immunoblotting with anti-p133 peptide antibody (α p133Ab) at a 1:100 dilution was performed using the ECL system as described by the manufacturer (Amersham).

Immunofluorescence and Electron Microscopy. Early logarithmic-phase cells were prepared for immunofluorescence with monoclonal antibody mAb414 and 4',6-diamidino-2-phenylindole (DAPI) and for EM exactly as described (8, 14).

Strains and Plasmids. The yeast strains used in this study were modifications of DF5 (17); *MATa/MAT α trp1-1/trp1-1 ura3-52/ura3-52 his3- Δ 200/his3- Δ 200 leu2-3,112/leu2-3,112 lys2-801/lys2-801*. All DNA manipulations were essentially as described (18). *NUP133* was isolated from a yeast genomic library by screening with a 1-kb PCR product amplified from yeast genomic DNA by using primers from the published sequence (19, 20). A 4.1-kb fragment, including the coding sequence and 492 bp of 5' and 175 bp of 3' flanking sequence, was subcloned into pIC20R (ref. 21; generating pLP-2) and the CEN/ARS plasmid, pRS316 (ref. 22; generating pLP-3).

Disruption of *NUP133*. A 234-bp *Spe* I-*Eco*RV fragment from pLP-2 (corresponding to amino acids 98–176) was replaced by a 1.8-kb *Xba* I-*Eco*RV fragment encoding the *HIS3* gene (generating pLP-4). Linearized pLP-4 was introduced into the diploid strain DF5a/ α , and *HIS*⁺ transformants selected (23). Targeted integration was verified by Southern analysis. Sporulation and dissection of the resulting strain were as described (24). Yeast strains were maintained in YPD or synthetic minimal medium supplemented with the appropriate amino acids and glucose (24).

RESULTS

Highly Enriched NPC Fractions Contain a Protein of 133 kDa. An enrichment procedure for the isolation of NPCs from yeast has been developed (4). Many individual polypeptides

Abbreviations: NPC, nuclear pore complex; ORF, open reading frame; DAPI, 4',6-diamidino-2-phenylindole.

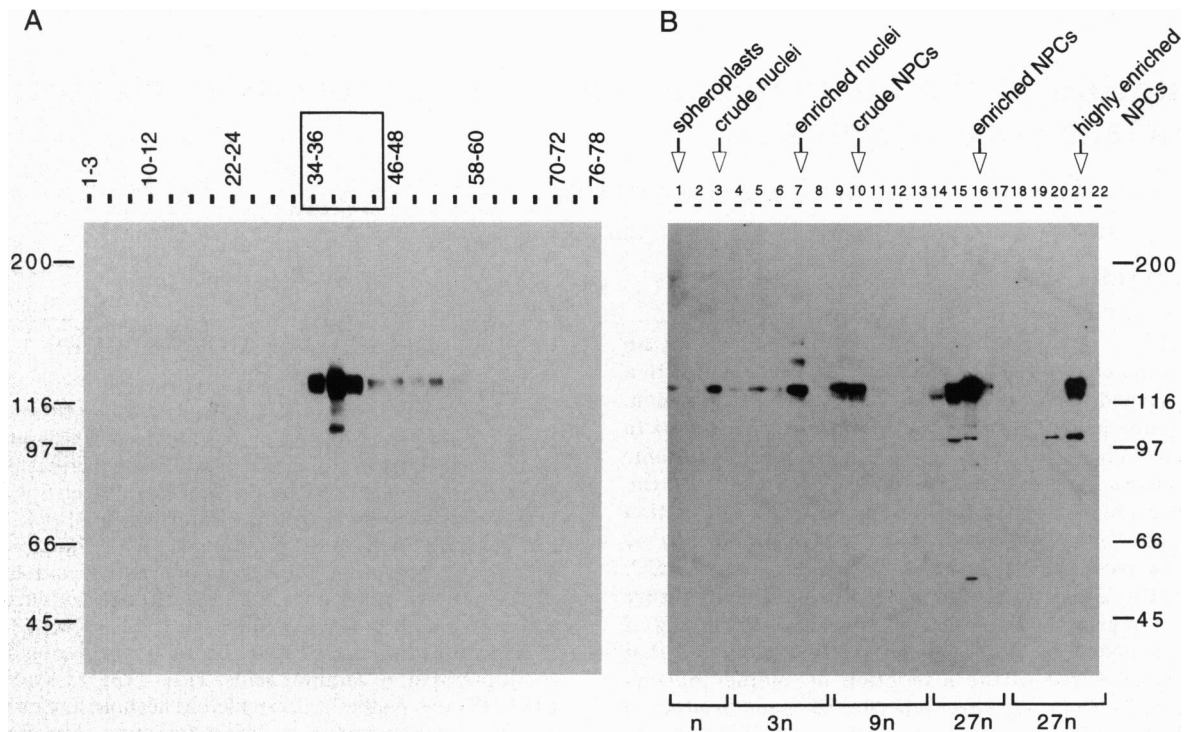


FIG. 1. p133 coenriches with the NPC. (A) Highly enriched NPC fraction was separated by ion-exchange chromatography. Unbound proteins were further separated by reverse-phase HPLC and SDS/PAGE (4). After immunoblotting and incubation with α p133Ab, antibody binding was visualized by using ECL. Numbers above the lanes indicate HPLC fractions, and boxed lanes indicate the fractions from which the 130-kDa protein was isolated. (B) Proteins from each fraction of the NPC-enrichment procedure (4) were separated by SDS/PAGE, immunoblotted with α p133Ab, and visualized by using ECL. NPC-containing fractions are indicated by arrows. The number of cell equivalents of protein loaded in each lane is indicated below the gel (the amount of protein in lane 1 has been set to 1n; ref. 4). The positions of molecular mass standards (in kDa) are indicated to the left of A and the right of B.

contained in this fraction represent candidate nucleoporins. These proteins were further fractionated by ion-exchange chromatography, reverse-phase HPLC, and SDS/PAGE (4). A doublet of approximately 130 kDa contained in HPLC fractions 34–45 was selected for partial amino acid sequence analysis. Comparison of the obtained amino acid sequence with protein data bases (EMBL and GenBank) revealed identity with a single open reading frame (ORF), YKR402/YKR082w, located on chromosome XI of *Saccharomyces cerevisiae* (20). This ORF encodes a protein of 133,448 Da (1157 amino acids), termed p133, in agreement with the estimated molecular mass of the protein obtained from the NPC fraction. All peptide sequences obtained from the 130-kDa doublet were encoded by this ORF and corresponded to amino acids 107–115, 195–201, 401–408, and 1089–1109. Anal-

ysis of the amino acid sequence revealed no significant similarities with other known proteins.

Antibodies were generated against a peptide corresponding to amino acids 1121–1135 of p133. The resulting antiserum was affinity purified by using the same peptide. To determine whether the antibody specifically recognized the 130-kDa doublet isolated from the highly enriched NPC fraction, proteins from all the HPLC fractions (4) were separated by SDS/PAGE, transferred to nitrocellulose, and probed with the anti-peptide antibodies (α p133Ab; Fig. 1A). The antibodies reacted specifically with a 130-kDa doublet contained in HPLC fractions 34–45 (Fig. 1A, boxed)—i.e., those fractions from which protein sequence data had been obtained. There was no reaction with preimmune serum (data not shown). Thus, the identified ORF corresponds to the protein present

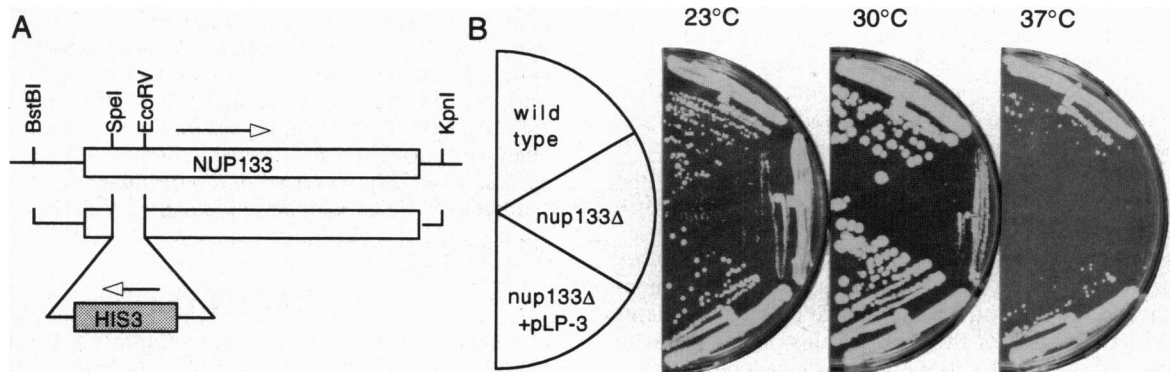


FIG. 2. Disruption of *NUP133*. (A) Schematic representations of *NUP133* and the *NUP133* disruption by *HIS3* are shown. Arrows indicate the direction of transcription of *NUP133* and *HIS3*. (B) DF5a cells (wild type), cells with the *nup133* disruption (*nup133* Δ), and *nup133* Δ cells complemented with a *NUP133*-containing plasmid (pLP-3) were streaked out in the sector pattern shown at the left and grown at the temperatures indicated for 4 days.

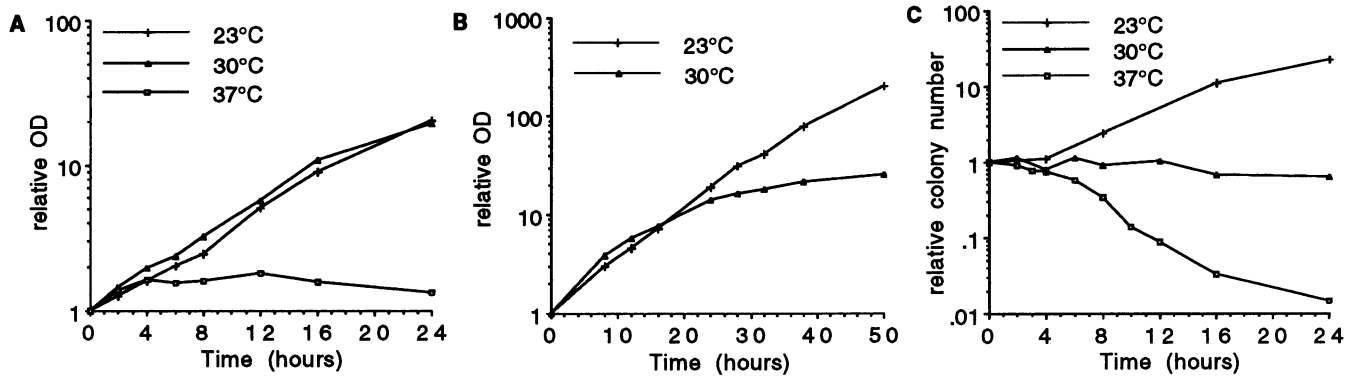


FIG. 3. Disruption of *NUP133* affects cell growth and viability. *nup133Δ* cells were grown in liquid medium at 23°C, 30°C, or 37°C. Growth was monitored by periodically measuring the OD at 600 nm over 24 h (A) or over 50 h (B). (C) Number of viable cells in cultures grown as in A was determined by plating aliquots of cells on YPD at 23°C and counting colonies after 4 or 5 days. The starting OD and colony number have been set equal to 1.

in the highly enriched NPC fraction. The antibodies recognized both bands of the 130-kDa doublet. It is most likely that the presence of these two bands represents proteolytic degradation of p133 during cell fractionation. (Note the presence of only one band in the early phases of cell fractionation, Fig. 1B.) Minor bands detected in some fractions are probably also proteolytic degradation products.

p133 Coenriches with NPCs. If p133 is indeed a nucleoporin, it should coenrich with NPCs during cell fractionation. The NPC enrichment procedure begins with whole yeast spheroplasts, which are fractionated through several purification steps to yield highly enriched NPCs (4). Analysis of fractions collected throughout the procedure showed that no non-NPC proteins coenriched with the NPC-containing fractions, while all but one NPC protein coenriched with the highly enriched NPC fraction (4).

Proteins from all of the fractions (from total cell lysate to highly enriched NPC fractions) were separated by SDS/PAGE, transferred to nitrocellulose, and immunoblotted with α p133Ab (Fig. 1B). As with similar immunoblots for other NPC proteins (4), p133 coenriched with the NPC, indicating that p133 is a component of the NPC. On the basis of this evidence, coupled with the p133 disruption phenotype (see below), we propose to term p133 Nup133p, in agreement with nomenclature for other yeast nucleoporins (8).

Disruption of *NUP133*. *NUP133*, including 492 bp of upstream sequence likely to contain the promoter, was isolated from a yeast genomic library. To determine the phenotype associated with disruption of this gene, the *HIS3* gene was inserted 293 bp downstream from the translational start of *NUP133* in the reverse orientation relative to *NUP133* (Fig. 2A). *HIS⁺* transformants were verified by Southern analysis and sporulated, and the tetrads were dissected. In all cases the *HIS⁺* marker cosegregated 2:2 with a severe growth defect. *his⁻* segregants formed colonies after 2 days, whereas *HIS⁺* segregants were visible after 5–7 days. To investigate this growth defect further, the growth rate and viability of *nup133Δ*-disrupted cells (*nup133Δ*) at different temperatures were examined. *nup133Δ* cells (strain YLP1) and wild-type cells were streaked on YPD and incubated at 23°C, 30°C, or 37°C. At all three temperatures wild-type cells formed colonies after 2 days. The *nup133Δ* strain was temperature sensitive for growth. These cells formed colonies after 3 or 4 days at 23°C, 4 or 5 days at 30°C, and not at all at 37°C (data not shown). Transformation of the *nup133Δ*-disrupted strain with the wild-type *NUP133* gene, carried on plasmid pLP-3, rescued this temperature-sensitive growth defect, demonstrating that the phenotype was a result of the *nup133* disruption. (Fig. 2B demonstrates the relative difference in colony size and number of the wild-type, *nup133Δ*, and *NUP133* cells grown for 4 days.

The doubling times of wild-type cells (DF5a/ α) and diploid *nup133Δ* cells (strain YLP3) grown at 23°C, 30°C, and 37°C were assessed by measuring the OD at 600 nm. Wild-type cells exhibited doubling times of 90 min at 30°C, 140 min at 37°C, and 160 min at 23°C. As expected, the growth rate of the *nup133Δ* cells was greatly reduced. At both 23°C and 30°C the doubling time was 270 min over a 24-h period (Fig. 3A). *nup133Δ* cells doubled once at 37°C and then ceased to grow. When *nup133Δ* cells were grown at 30°C for longer periods, they exhibited a severe slowing of growth after 24 h. This was not detected in *nup133Δ* cells grown at 23°C (Fig. 3B).

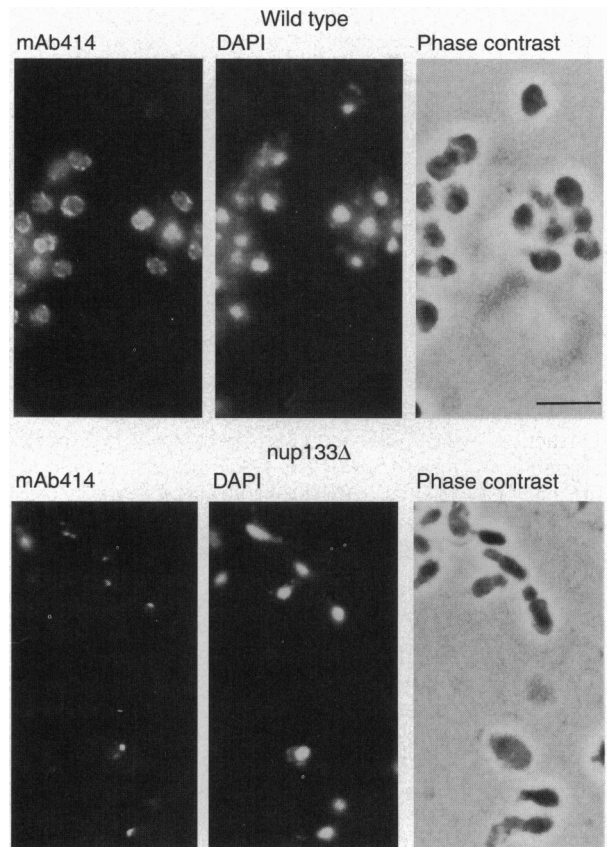


FIG. 4. Immunofluorescent localization of mAb414-reactive nucleoporins is altered in *nup133Δ* cells. DF5a/ α (wild type) and YLP3 (*nup133Δ*) cells were fixed and incubated first with mAb414, and then with fluorescein isothiocyanate (FITC)-conjugated goat anti-mouse immunoglobulin. The coincident DAPI staining and phase-contrast images are shown. (Scale bar = 5 μ m.)

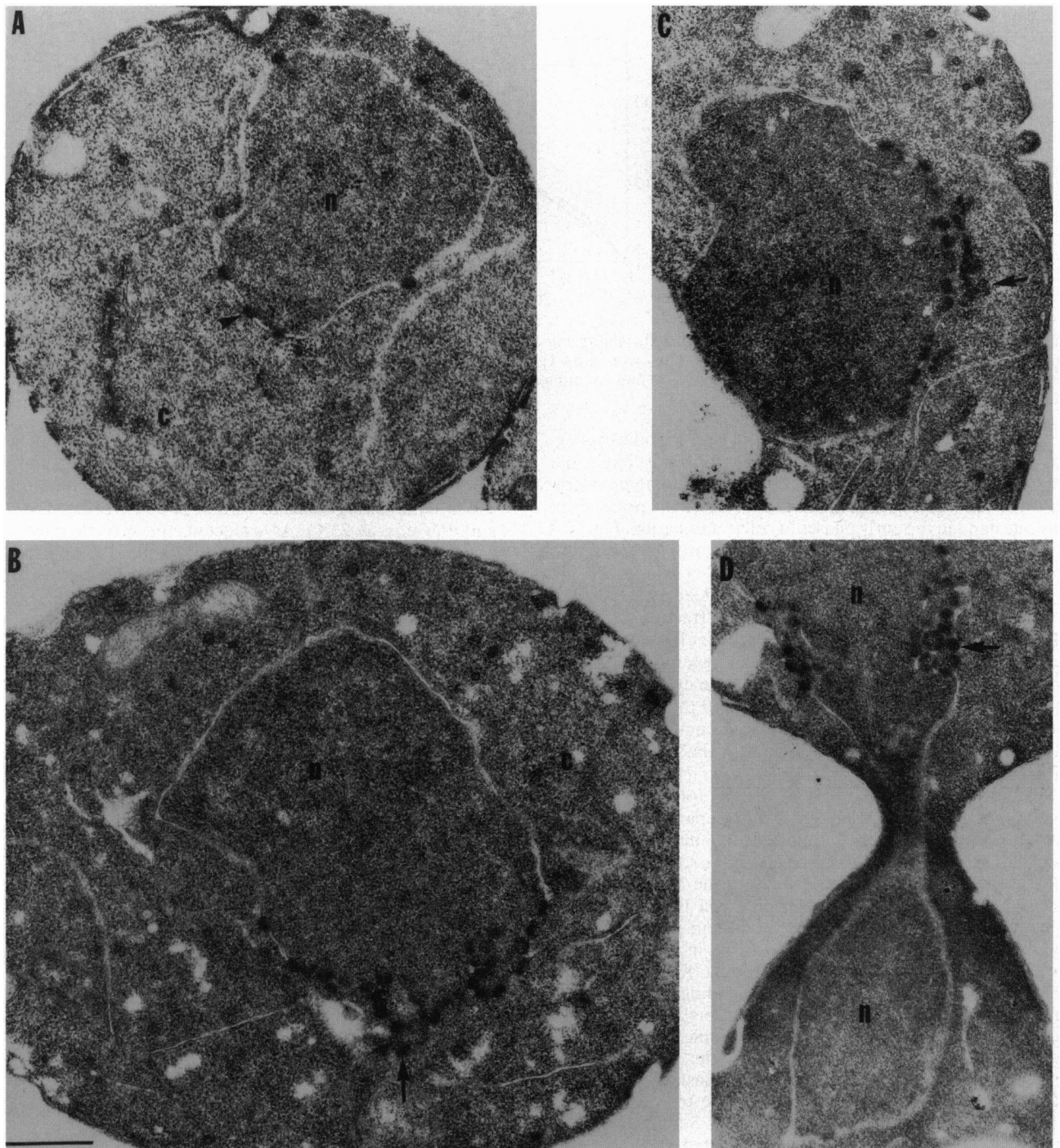


FIG. 5. Electron microscopic analysis of the nuclear envelope in *nup133Δ* cells. Haploid DF5a (A) and *nup133Δ* (B–D) cells were grown to early logarithmic phase at 23°C and processed for EM. Arrows indicate NPCs; n, nucleus; c, cytoplasm. (Scale bar = 0.5 μ m.)

Cell viability at these temperatures was determined by measuring colony-forming ability. Cells were grown as in Fig. 3A over a 24-h period. At specific time points, aliquots were removed, plated, and grown at 23°C, and the resulting colonies were counted (Fig. 3C). *nup133Δ* cells grown at 23°C (and wild-type cells grown at 23°C, 30°C, and 37°C; data not shown) showed no decrease in viability over time; the number of colonies increased at the same rate as the OD (Fig. 3C). In contrast, the colony-forming ability of *nup133Δ* cells grown at 30°C did not reflect the increase in OD. The number of colonies increased approximately 2-fold over 6 h and decreased thereafter (Fig. 3C). The OD of these cultures appeared to increase by 20-fold over 24 h (Fig. 3A). When a culture of *nup133Δ* cells was grown at 37°C, the number of

viable cells decreased. After 24 h <2% of the starting number of cells were viable (Fig. 3C). This indicated that the 37°C shift was lethal, as the cells could not be rescued by replating them at the permissive temperature (23°C).

Immunolocalization of Nucleoporins Is Altered by the Disruption of *NUPI33*. The distribution of NPCs was examined by indirect immunofluorescence in the diploid *nup133Δ* cells. Monoclonal antibody mAb414 (25), which reacts with a subset of six nucleoporins (4) but does not react with Nup133p, was used to probe wild-type (DF5a/ α) and *nup133Δ* cells grown at 23°C. In the wild-type cells, immunofluorescent staining formed a punctate pattern that localized to the nuclear periphery, typical of normal NPC distribution (Fig. 4). In the *nup133Δ* cells, this localization was abolished and the immu-

nofluorescence signal was confined to a spot in one area of the nuclear periphery (Fig. 4). DAPI staining of these cells appeared normal; however, the morphology of many of the *nup133Δ* cells was altered. Many cells appeared to be larger than the wild type, and some cells appeared more elongated, with one or more elongated buds. *nup133Δ* cells were also grown for several hours at 30°C and 37°C. At 30°C most of the cells demonstrated an altered morphology, with many large cells and cells with very elongated and multiple buds. At 37°C, the cultures showed very large, paired cells with large vacuoles and cell debris (data not shown).

Disruption of *NUP133* Leads to Ultrastructural Abnormalities at the Nuclear Envelope. Wild-type (DF5a) and *nup133Δ* cells (strain YLP1) were examined by thin-section EM after growth in rich medium at 23°C. As expected, NPCs of wild-type cells were spaced at discrete intervals around the nuclear envelope (Fig. 5A). However, in the *nup133Δ* cells, NPCs were clustered in one or two areas of the nuclear envelope. This phenotype was observed in most sections where NPCs were visible. In most cases, the NPCs appeared to be densely clustered, as though the nuclear envelope was folding or invaginating (Fig. 5B). In some cells, the NPCs appeared to be in two parallel rows (Fig. 5C). At 23°C, the *nup133*-disrupted cells appear to bud readily, and the nucleus can be seen entering the bud even when NPCs are exhibiting a clustered phenotype (Fig. 5D).

DISCUSSION

We have isolated proteins from a highly enriched preparation of NPCs. One protein, with an estimated molecular mass of 130 kDa, was identified by protein sequencing as a previously published, uncharacterized ORF of 133 kDa. We have identified this protein as a nucleoporin on the basis of two independent lines of evidence. First, monospecific antibodies directed against this protein show its coenrichment with yeast NPCs during their preparation as a highly enriched fraction. Second, disruption of the gene encoding this protein results in an NPC-specific phenotype. We propose that this protein be named Nup133p, following standard nomenclature. Examination of the amino acid sequence of Nup133p does not reveal any sequence similarities with other nucleoporins from yeast or vertebrates, and this protein does not appear to contain any repeating sequence motifs.

Although the protein could be detected by immunoblotting, immunolocalization of the protein by the antibody or through epitope tagging was not successful. The biochemical and genetic data in themselves are sufficient to identify Nup133p as an NPC protein, however, its immunolocalization will still be required to define its sublocalization to discrete functional domains within the NPC.

Disruption of this protein led specifically to abnormalities in NPC localization and nuclear envelope structure. Immunofluorescent localization of other NPC proteins demonstrated that the NPCs localized to one or two spots within the nuclear periphery. Ultrastructural analysis demonstrated that large numbers of NPCs were clustering in one area of the nuclear envelope. The envelope may be folding and invaginating in these regions. Disruption of *NUP133* also led to growth defects, with cell growth and viability appearing to decrease with increased temperature.

At 23°C, although the NPCs appeared to be clustered at one site in the nuclear envelope, logarithmic growth and viability indicated that new NPCs can be assembled and nucleocytoplasmic transport can take place. At 37°C, however, cells became inviable after one doubling. This may suggest that, at this temperature, nucleocytoplasmic transport cannot occur or that more NPCs cannot be assembled, leading to the death of

these cells. Our unpublished data show that after 3 h of growth at 37°C, NPCs also exhibit a clustering phenotype, implying that the clustering phenotype alone does not lead to the loss in viability and that other factors must be involved.

At the intermediate temperature, 30°C, the cells cannot sustain growth over long periods of time. It appears that these cells are unable to complete the budding process, but it is not yet known if this is directly related to a deficiency in the number or function of NPCs.

Abnormalities in the nuclear envelope have been observed in disruptions of two other nucleoporins, Nup116p and Nup145p (refs. 14 and 10, respectively). In the case of *nup116*, a similar slow-growth phenotype and loss of viability at 37°C was observed. However, the sealed pores and electron-dense material observed in those cells at 37°C were not detected in *nup133*-disrupted cells at 23°C (14). The clustering-NPC phenotype observed here appears similar to that seen in the *nup145* disruption, suggesting that this is an NPC-specific phenotype (10). The effect seems more exaggerated in the *nup133* strain, as the disruption appears to affect both cell growth and viability. There is no sequence similarity between these genes; however, it is possible that they may have overlapping functions within the NPC structure. The clustering of NPCs suggests that these proteins may be important for maintaining the position of the pore within the envelope, possibly by interacting with non-NPC proteins or by preventing the association of NPCs with one another. The appearance of folding and invagination of the nuclear envelope may suggest that these nucleoporins or the NPC as a whole plays a role in maintaining the architecture of the nuclear envelope. Understanding these phenomena may also help elucidate the mechanism of NPC assembly and the insertion of NPCs into the nuclear envelope.

We especially thank Helen Shio for her assistance with the electron microscopy and Joseph Fernandez at the Rockefeller University Protein Sequencing Facility. We thank Drs. Susan Smith, John Aitchison, and David Wotton for critical reading of the manuscript.

1. Rout, M. P. & Wente, S. R. (1994) *Trends Cell Biol.* **4**, 357–365.
2. Miller, M., Park, M. K. & Hanover, J. A. (1991) *Physiol. Rev.* **71**, 909–949.
3. Forbes, D. J. (1992) *Annu. Rev. Cell Biol.* **8**, 495–527.
4. Rout, M. P. & Blobel, G. (1993) *J. Cell Biol.* **123**, 771–783.
5. Davis, L. I. & Fink, G. R. (1990) *Cell* **61**, 965–978.
6. Loeb, J. D., Davis, L. I. & Fink, G. R. (1993) *Mol. Biol. Cell* **4**, 209–222.
7. Nehrbass, U., Kern, H., Mutvei, A., Horstmann, H., Marshallsay, B. & Hurt, E. C. (1990) *Cell* **61**, 979–989.
8. Wente, S. R., Rout, M. P. & Blobel, G. (1992) *J. Cell Biol.* **119**, 705–723.
9. Wimmer, C., Doye, V., Grandi, P., Nehrbass, U. & Hurt, E. C. (1992) *EMBO J.* **11**, 5051–5061.
10. Wente, S. R. & Blobel, G. (1994) *J. Cell Biol.* **125**, 959–969.
11. Fabre, E., Boelens, W. C., Wimmer, C., Mattaj, I. W. & Hurt, E. C. (1994) *Cell* **78**, 275–289.
12. Grandi, P., Doye, V. & Hurt, E. C. (1993) *EMBO J.* **12**, 3061–3071.
13. Wozniak, R. W., Blobel, G. & Rout, M. P. (1994) *J. Cell Biol.* **125**, 31–42.
14. Wente, S. R. & Blobel, G. (1993) *J. Cell Biol.* **123**, 275–284.
15. Fernandez, J. M., DeMott, D., Atherton, D. & Mische, S. M. (1992) *Anal. Biochem.* **201**, 255–264.
16. Fernandez, J., Andrews, L. & Mische, S. M. (1994) *Anal. Biochem.* **218**, 112–117.
17. Finley, D., Ozkaynak, E. & Varshavsky, A. (1987) *Cell* **48**, 1035–1046.
18. Sambrook, J., Fritsch, E. F. & Maniatis, T. (1989) *Molecular Cloning: A Laboratory Manual* (Cold Spring Harbor Lab. Press, Plainview, NY), 2nd Ed.
19. Rose, M. D., Novick, P., Thomas, J. H., Botstein, D. & Fink, G. R. (1987) *Gene* **60**, 237–243.
20. Garcia-Cantelejo, J., Baladron, V., Esteban, P. F., Santos, M. A., Bou, G., Remacha, M. A., Revuelta, J. L., Ballesta, J. P. G., Jimenez, A. & Del Rey, F. (1994) *Yeast* **10**, 231–245.
21. Marsh, J. L., Erfle, M. & Wykes, E. J. (1984) *Gene* **32**, 481–485.
22. Sikorski, R. S. & Hieter, P. (1989) *Genetics* **122**, 19–27.
23. Ito, H., Fukuda, Y., Murata, K. & Kimura, A. (1983) *J. Bacteriol.* **153**, 163–168.
24. Sherman, F., Fink, G. R. & Hicks, J. B. (1991) *Methods in Yeast Genetics* (Cold Spring Harbor Lab. Press, Plainview, NY).
25. Davis, L. I. & Blobel, G. (1986) *Cell* **45**, 699–709.